

LIGHT SCATTERING BY FREE ELECTRONS AND ELECTRON-PHONON COUPLED MODES IN SEMICONDUCTORS

Manuel Cardona

Max-Planck-Institut für Festkörperforschung
 Heisenbergstr. 1
 7000 Stuttgart 80
 Federal Republic of Germany

Light scattering in heavily doped Ge, Si, and GaAs is discussed with emphasis on the interaction between phonons and electronic continua.

I. Introduction

Scattering by electronic excitations represents the simplest type of light scattering process in solids. It has first (A^2) and second ($A.p$) order perturbation contributions [1] while the scattering by phonons corresponds to processes of at least third order (twice $A.p$ and once the electron-phonon interaction). With the exception of scattering by electrons bound to impurities [1,2] and in magnetic fields [3] the scattering of light by electrons produces broad spectra, in contrast with the sharp spectra of phonons. Hence little experimental attention has been given to scattering by electronic continua and, in particular, to scattering by interband transitions across the lowest gap of semiconductors. These transitions are allowed for photon absorption and, because of parity (Ge) or quasi-parity (GaAs), forbidden for light scattering. While considerable theoretical attention has been given to these processes [4], only recently antistokes interband scattering has been observed in GaSb [5] and Stokes scattering in InSb [6]. Intraband scattering by free carriers (Fig. 1) has received attention as it can interfere quantum mechanically with phonon scattering [7-11]. From an analysis of the observed (Fano-) line shapes electron-phonon interaction constants are obtained (magnitude and sign). Strong electron-phonon interaction also occurs for Raman active LO-phonons in polar materials [12,13]. It leads to dispersive mixed phonon-plasmon modes [14,15]. We discuss these phenomena for Ge, Si, and GaAs, together with resonant spin-flip scattering in GaAs and low frequency scattering by multicomponent plasmas in n- and p-type Si.

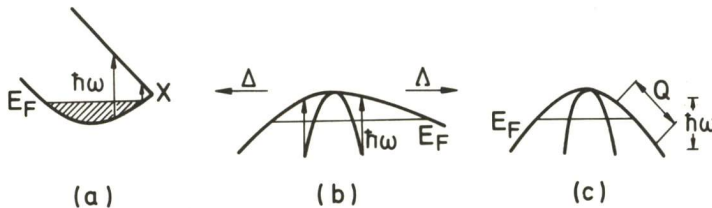


Fig. 1
 Intraband continua: (a) n-Si, (b) p-Ge, Si, (c) GaAs, p-Ge.

II. Intraconduction-Band Continuum in n-Type Si

Figure (2) shows the first and second order Raman spectra of two heavily phosphorus doped Si samples compared with that of intrinsic Si [8]. The spectrum of the heavily doped samples is basi-

cally the same as the intrinsic one, except for a broad background which can be associated with the transitions of Fig.(1a). The first order phonon peak at $\sim 520 \text{ cm}^{-1}$ interferes with the background, constructively below 520 cm^{-1} and destructively above. The dashed lines represent fits to the asymmetric first order phonon with a Fano expression:

$$I(e) = (q+e)^2/1+e^2; \text{ with } e = (\omega-\omega_0-\Delta\omega_0)/\Gamma \text{ and } q = (VT_p/T_e+\Delta\omega_0)/\Gamma. \quad (1)$$

The width Γ contains two parts, the intrinsic width Γ_i and the imaginary part of the self energy [9]:

$$\Gamma = \Gamma_i + \pi V^2 D(\omega); \Delta\omega_0 = V^2 \int D(\omega') \left(\frac{1}{\omega-\omega'} + \frac{1}{-\omega-\omega'} \right) d\omega', \quad (2)$$

where $D(\omega)$ is the density of continuum states and V the matrix element for their interaction with the phonon. It can be written in terms of the deformation potential D_0 (usually given in eV) [9]:

$$V = \frac{D_0}{a} (\pi a^3 / M \omega_0)^{1/2} \quad (3)$$

where a is the lattice constant and M the atomic mass. Γ and $\Delta\omega_0$ can be easily evaluated from Eqs. (2) and (3) and the masses of n-Si provided D_0 is known. The experimental Γ and $\Delta\omega_0$ are in good agreement with simple calculations of D_0 ($D_0 = -8.1 \text{ eV}$). These calculations also yield T_e , T_p and their relative sign. Hence q and its sign can be determined theoretically (no computer calculations needed).

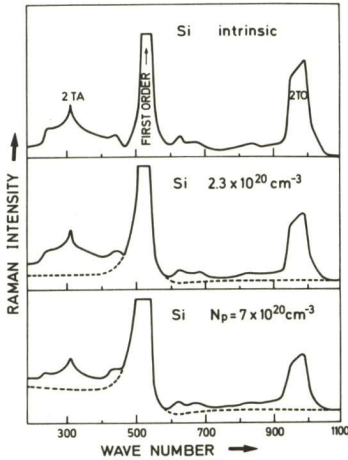


Fig. 2

First and second order Raman scattering of n-type Si samples. Dashed line: fit with a Fano-expression [8]

III. Intravalence-Band Continuum

1. p-Type Si. Figure (3) shows the first order Raman spectra of four heavily B-doped Si samples and the corresponding fits with eq. (1). A discrete-continuum interference is also apparent. The continuum has been assigned to the transitions of Fig.(1b). The relative strength of the electronic continuum, and thus q , depends on laser frequency. The reason is the stronger resonance of the scattering by phonons ($\propto |T_p|^2$) as the direct gap of Si (3.3 eV)

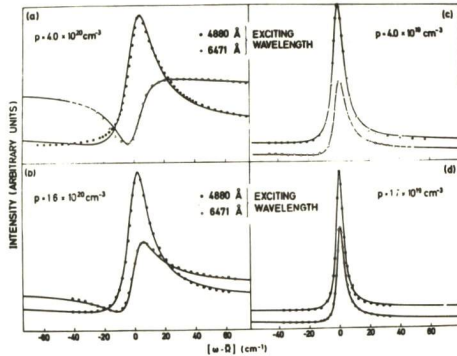


Fig. 3

Raman scattering by optical phonons in p-type Si [7]

is approached. The Fano parameters obtained from the fits of Fig.(3) must be expressed with a modified form of Eq. (2): because of the degeneracy of the valence bands the wave functions, and thus V , depend on the direction of k . V must be replaced by a k -average, to be obtained numerically [16], proportional to the deformation potential constant d_0 (in eV). The results for $d_0 = 27\text{eV}$ and $T = 77\text{K}$ are shown in Fig. (4). Agreement with experiment is good except for the sign reversal of $\Delta\omega$ predicted for low doping (the result of the fact that at this doping the continuum lies mostly below ω). This reversal disappears when the calculation is performed at 300K. Impurity scattering probably broadens the continuum and eliminates the sign reversal of Fig.(4). We note that the discrete-continuum interference of Fig.(3) is destructive below ω_0 , opposite to the case of Fig.(2): the sign of \bar{d} must be positive. Band structure calculations yield $d_0 = +27\text{ eV}$ [17].

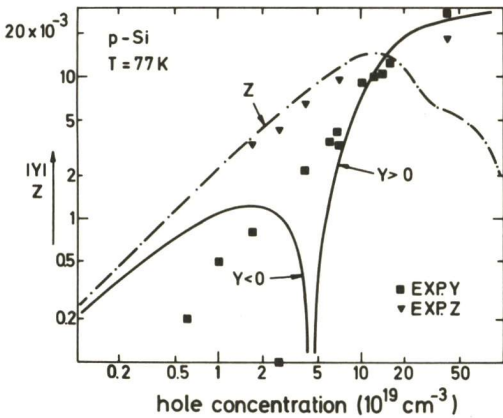


Fig. 4

Normalized real and imaginary parts of the self energy of the phonons in p-type Si: $Y = -(\Delta\omega_0/\omega_0)$, $Z = \Gamma/\omega$ [16]

2. p-Type Ge. For $N_D \approx 2 \times 10^{19} \text{ cm}^{-3}$ the intra-valence-band continuum of Fig.(1b) lies above the Raman phonon frequency. One must also consider in eqs. (2) electronic transitions from occupied to empty heavy hole states (Fig.(1c)). The density of states for these transitions, basically single particle excitations of a free electron gas, depends on the \vec{Q} -vector transfer (i.e. on the Q of the phonons, see Fig.(5)). The magnitude of this \vec{Q} -vector equals $4\pi n/\lambda_L$, where n is the refractive index and λ_L the laser wavelength. Hence it is possible to vary the \vec{Q} -vector, and thus the density of states, by varying the laser frequency [10]. The range of Q -vectors covered in existing experiments is indicated in Fig.(5): the corresponding phonons lie below (above) the intraband continuum at low (high) hole concentrations. Eqs. (2) yield parameters $\Delta\omega$, Γ , and q which depend strongly on λ_L . Experimental results are shown in Fig.(6) together with a fit for $d_0 = 32\text{ eV}$ (band calculations yield $d_0 = +33\text{ eV}$ [18]).

3. p-Type GaAs. The average heavy hole mass is $\approx 0.6m_0$, much larger than for p-Ge. As a result in Fig.(5) (\vec{Q}, ω) is well outside the free particle continuum for all standard laser frequencies. ω_0 is also outside the light hole \rightarrow heavy hole continuum. Nevertheless we find an increase in Γ with Zn-doping and an asymmetric line width [10] ($q = -10$ for $N_D = 9 \times 10^{19} \text{ cm}^{-3}$). The continuum arises from transitions with \vec{Q} -nonconservation induced by the Zn impurities [19].

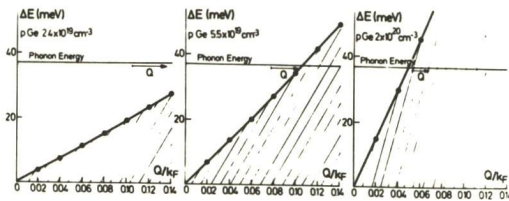


Fig. 5

Single particle excitations within the heavy hole band of p-Ge [10]

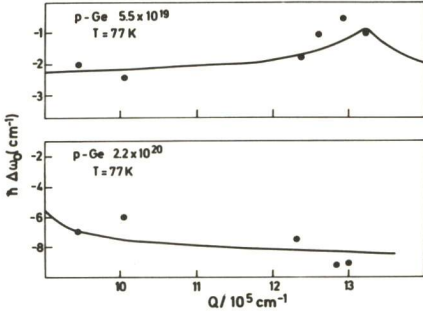


Fig. 6

Real part of phonon self energy in p-Ge and fit with $d_0 = 32$ eV

4. p-Type Si: B-Induced Local Mode.

Two local modes appear on account of the two B-isotopes (B_{11} and B_{10}) [20,21]. The q-parameters of the local modes have the same sign as for the Si-phonon but are smaller. The Raman cross-section per atom is much larger for the local mode than for the Si-phonon. These results are discussed at this meeting by Chandrasekhar et al.

Similar effects, in particular a renormalization $\Delta\omega_0$ of the phonon frequency, occur for interband transitions in small gap semiconductors. For zincblende-type materials the deformation potential for optical coupling across the E_0 gap is nearly zero [22]. In the IV-VI materials (GeTe) this coupling produces large softening of the TO phonons [23] and may be responsible for a ferroelectric transition [24].

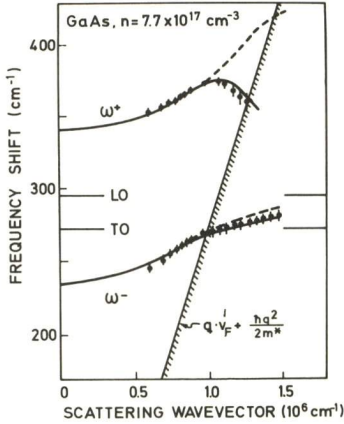


Fig. 7

Dispersion of the coupled LO-phonon-plasmon modes in n-GaAs, allowed configuration. Dashed line: from Eq. (6). Solid line: dashed line convoluted to include finite penetration depth [25].

IV. Coupled LO Phonons and Plasmons

1. n-GaAs. We consider first the scattering by free electron excitation in a single valley system such as GaAs. The electron-photon coupling has the form:

$$H_{ep} = H_{ep}^{(1)} + H_{ep}^{(2)}; \quad H_{ep}^{(1)} = \frac{e}{2mc} \vec{A}_S \cdot \vec{p} + \frac{e}{2mc} \vec{A}_L \cdot \vec{p}; \quad H_{ep}^{(2)} = \frac{e^2}{2mc^2} \vec{A}_S \cdot \vec{A}_L \quad (3)$$

where \vec{A}_S and \vec{A}_L are the vector potentials of the incident and scattered light, respectively and \vec{p} the linear momentum operator. $H^{(2)}$ acts in first order and $H^{(1)}$ in second order. Away from resonances both terms can be combined by using k.p theory: One obtains an effective hamiltonian $H^{(2)}$ [1]:

$$H_{ep} = \frac{e}{2c} \vec{A}_S \cdot \frac{1}{m^*} \vec{A}_L, \quad (4)$$

where $\frac{1}{m^*}$ is the effective mass tensor. Equation (4) represents a longitudinal perturbation which produces a charge density wave of amplitude proportional to ϵ_e^{-1} , where ϵ_e is the dielectric function including the free electrons. The scattering cross section is thus proportional to the "loss function" $\text{im } \epsilon_e^{-1}$. This function peaks at the plasma frequency ω_p ($\epsilon_e^{-1}(\omega_p) = 0$) and shows little strength at low frequencies $\omega \ll \omega_p$: Raman scattering does not couple to the low frequency excitations of Fig.(5) as they are "screened out" by the electron gas. In the presence of optically active phonons one must

consider the total dielectric constant [13-15]:

$$\epsilon(\vec{q}, \omega) = 4\pi\chi_e(\omega, q) + (\omega_L^2 - \omega^2) / (\omega_T^2 - \omega^2) \quad (5)$$

where χ_e is the polarizability of the free electrons. If χ_e is real (or if the imaginary part is small), the scattering yields two peaks at the "coupled mode" frequencies ω_+ and ω_- which fulfill $\epsilon_r(\vec{q}, \omega^\pm) = 0$. As the losses become higher, the peak positions must be obtained from the response functions:

$$\frac{d^2\sigma}{d\Omega d\omega} \propto - \frac{(\omega_0^2 - \omega^2)^2}{(\omega_T^2 - \omega^2)^2} \text{im} \frac{1}{\epsilon(\vec{q}, \omega)} \quad (6)$$

for an allowed LO phonon scattering configuration ($\omega_0^2 = \omega_T^2(1+C)$, where C is the Faust-Henry coefficient) and

$$\frac{d^2\sigma}{d\Omega d\omega} = - \left(\frac{\omega_L^2 - \omega^2}{\omega_T^2 - \omega^2} \right)^2 \text{im} \frac{1}{\epsilon(\vec{q}, \omega)} \quad (7)$$

for a parallel-parallel forbidden LO configuration. The experimental ω_+ and ω_- exhibit a Q-dependence which is observed as the laser wavelength is changed (see Fig.(7)). In order to account for the dispersion one evaluates the maxima of eqs. (6) and (7) using for $\chi_e(\vec{q}, \omega)$ the Lindhard function modified to include the effect of collisions and finite temperature. The results are shown by the dashed line in Fig. 7 [25]. The disagreement with the experiments in the region of Landau damping is due to the finite penetration depth: at large Q's the mixed modes are broad and one sees mainly the peaks for lower Q through the admixture produced by the Q-width. The solid lines, which account well for the observed data, are obtained by convoluting eq. (7) with a Lorentzian of width α (the absorption coefficient). It has been recently pointed out [26] that the cumbersome numerical integrations used for evaluating $\chi_e(\vec{q}, \omega)$ are not necessary. The experimental data in the region of Fig.(7) can be fitted equally well by the simple expression [26]:

$$4\pi\chi_e = - \frac{\omega_p^2}{\omega^2 - DQ^2 + i\omega\omega_\tau} \quad (8)$$

where D is a diffusion constant and ω_τ the scattering frequency.

2. p-GaAs. Figure (8) shows the scattering for p-GaAs sample ($N_p = 9 \times 10^{19} \text{ cm}^{-3}$) in "forbidden LO" configuration [27]. The coupled modes which correspond to $Q = 4\pi n / \lambda_L$ are not observed. Instead, a broad and asymmetric line slightly below the LO-line of pure GaAs is seen. This line can be explained as ω_- for $Q \gg 4\pi n / \lambda_L$: the non-conservation of \vec{Q} would then be produced by impurity scattering [28]. The solid lines of Fig.(8A and B) were obtained by convoluting Eq. (7) with the square of a screened Coulomb potential:

$$V^2(Q) = [Q^2 + Q_{TF}^2]^{-2} \quad (9)$$

where Q_{TF} is the screening radius. In Fig.(8A), the convolution was carried out to a maximum $Q = 2Q_F$ ($Q_F =$ Fermi radius). In Fig.(8B) to $Q = 3Q_F$: this figure shows the experimental line plus a peak at $\omega = \omega_{LO}$ not seen in the experiments. Although no detailed calculations of this impurity-induced scattering have been performed, the cutoff introduced above can be justified as due to a decrease in the

cross section of Eq. (6) with increasing Q.

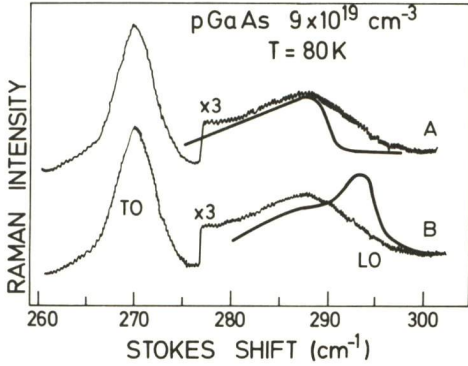


Fig. 8

Impurity induced Raman scattering in p-GaAs: The solid curves were calculated by convolution with the impurity potential (see text) [27].

Near a spin-orbit split gap, such as $E_0 + \Delta_0$ for n-GaAs, its derivation breaks down and one must go back to Eq. (3). Spin-flip scattering, which is not screened by the electron plasma, becomes possible for $\omega \ll \omega_p$ [29] (see Fig.(9)). This scattering has been profusely studied in the presence of a magnetic field [3,30] as it is the mechanism of the spin-flip laser. For $H=0$, however, it has received little experimental attention.

This spin-flip scattering exhibits a Lorentzian resonance around the $E_0 + \Delta_0$ gap shown in Fig.(10) together with the corresponding resonance of the ω^+ and ω^- mixed modes. Recently a calculation of the scattering lineshape without adjustable parameters has been published [32]. In this calculation, shown in Fig.(11) together with experimental results for $N_D = 6 \times 10^{18} \text{ cm}^{-3}$, the width of the spectrum for $\omega = Qv_F$ results from fluctuations in the impurity concentration.

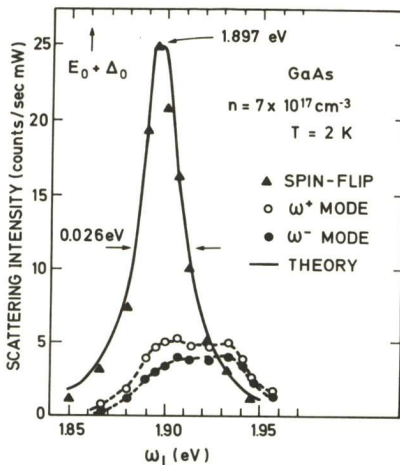
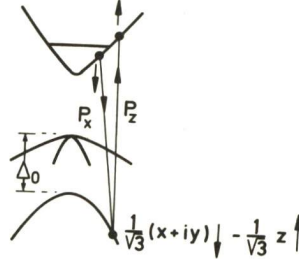


Fig. 10

Resonance of the spin-flip and the mixed mode scattering in n-GaAs. Solid line: Lorentzian fit.

Fig. 9

Spin-flip scattering near $E_0 + \Delta_0$ gap of n-GaAs



V. Spin-Flip Scattering

The hamiltonian of eq. (4) leads to a scattering peak near ω_p and no scattering for $\omega \ll \omega_p$: This hamiltonian, however, is only valid away from resonances.

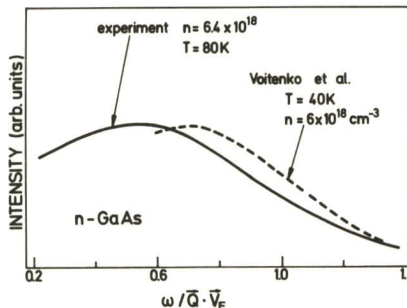


Fig. 11

Spin-flip scattering near $E_0 + \Delta_0$ for n-GaAs ($N_D = 6.4 \times 10^{18} \text{ cm}^{-3}$) and calculation by Voitenko et al. [32] ($Qv_F = 280 \text{ cm}^{-1}$)

VI. Scattering by Multicarrier Systems

1. n-Type Si. We may set up charge density fluctuations in the various valleys with no net charge density fluctuation. This type of excitation is not screened at low frequencies as it has no net charge. It is therefore expected to give low frequency scattering [33] which has been recently observed in n-Si [34] (see Fig.(12)). To test the nature of this scattering, we apply a stress along [001] which lowers the valleys along [001] with respect to those along [100] and [010] and thus transforms the multicarrier system into a one-component plasma. The low frequency tail is reduced by the stress (see Fig.(12)) thus proving that it is due to the multivalley nature of the plasma. The scattering cross section is given by [34]:

$$\frac{d^2\sigma}{d\omega d\Omega} \propto \frac{(1+n_\omega) \text{Im} \sum_{i < j} (\mu_i - \mu_j)^2 \bar{Q}_i \cdot \bar{Q}_j}{\hbar\omega(\hbar\omega + i\hbar\omega_\tau)}, \mu_i = \vec{A}_L \cdot \frac{1}{m_i} \cdot \vec{A}_S, \bar{Q}_i = \vec{Q} \cdot \frac{1}{m_i} \cdot \vec{Q}, \quad (10)$$

n_ω is the Bose-Einstein factor and $1/m_i^*$ the inverse mass tensor of valley i . The sum of Eq. (10) is extended to all components of the plasma.

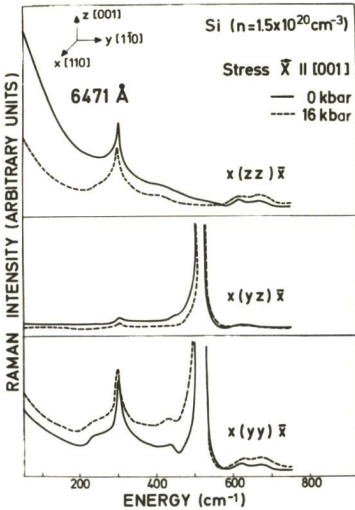


Fig. 12

Low frequency scattering due to intervalley fluctuations in n-Si: The scattering decreases under a uniaxial stress along [001][34].

$$\frac{d^2\sigma}{d\omega d\Omega} \propto \text{Im} \frac{(1+n_\omega)}{\hbar\omega(\hbar\omega + i\hbar\omega_\tau)} \iint_{E_F} [\mu(\vec{k}) - \mu(\vec{k}')]^2 dS_{\vec{k}} dS_{\vec{k}'}, \quad (11)$$

The integral of Eq. (11) represents the mean square fluctuation of the heavy hole mass around the Fermi surface. Although it should be evaluated numerically, it is possible to approximate it by a sum of the type of Eq. (10) including only groups of carriers along high symmetry directions. Such calculation yields for p-Si a low frequency scattering of mainly Γ_{25} symmetry, in agreement with experiment [35].

Equation (10) represents a rather complicated tensorial dependence of the scattering cross section: an eighth rank tensor contracted with the directions of \vec{A}_L , \vec{A}_S (twice each) and \vec{Q} (four times).

The experiments for n-Si do not agree with the selection rules derived from this tensorial dependence. They agree, however, with the result of removing Q_i and Q_j from Eq. (10). In view of the examples of violation of \vec{Q} conservation due to impurity scattering seen above we conclude that this violation is also effective in removing the $Q_{i,j}$ terms of Eq. (10).

2. p-Type Si. The hole band of Si is strongly warped and a wide distribution of hole masses is present. Thus carrier density fluctuations from regions of high mass to regions of low mass with no net charge fluctuation are possible. These fluctuations should also give unscreened scattering at low frequencies [35]. The scattering disappears, together with the warping when a uniaxial stress is applied. The cross section should be proportional to the generalized version of Eq. (10) [35]

M. CARDONA

- 1) See, for instance, M.V. Klein in: "Light Scattering in Solids", ed. by M. Cardona (Springer Verlag, Berlin, 1975), p. 147.
- 2) C.H. Henry, J.J. Hopfield, and L.C. Luther: Phys. Rev. Letters 17 (1966), 1492.
- 3) R.E. Slusher, C.C.N. Patel, and P.A. Fleury: Phys. Rev. Letters 18 (1967) 77.
- 4) D.L. Mills, R.F. Wallis, and E. Burstein in: "Light Scattering in Solids", ed. by M. Balkanski (Flammarion, Paris, 1971) p. 107.
- 5) G. Benz and R. Conradt: Phys. Rev. Letters 34 (1975) 1551.
- 6) J. Geurts and W. Richter in: "Physics of Semiconductors", ed. by B.L.H. Wilson (Institute of Physics, Bristol, 1979) p. 513.
- 7) F. Cerdeira, T.A. Fjeldly, and M. Cardona: Phys. Rev. B8 (1973) 4734.
- 8) M. Jouanne, R. Besserman, I. Ipatova and A. Subashiev: Solid State Commun. 16 (1975) 1047.
- 9) M. Chandrasekhar, J.B. Renucci, and M. Cardona: Phys. Rev. B17 (1978) 1623.
- 10) D. Olego and M. Cardona: Ref. 6, p. 1313.
- 11) M. Balkanski, K.P. Jain, R. Besserman, and M. Jouanne: Phys. Rev. B12 (1975) 328.
- 12) I. Yokota: J. Phys. Soc. Japan 16 (1961) 2075.
- 13) A. Mooradian and G.B. Wright: Phys. Rev. Letters 16 (1966) 999.
- 14) V.L. Gurevich, A.L. Larkin, and Yu.A. Firsov: Sov. Physics-Solid State 4 (1962) 131.
- 15) K. Murase, S. Katayama, Y. Ando, and H. Kawamura: Phys. Rev. Letters 33 (1974) 1481.
- 16) P. Lawaetz, Report Physics Laboratory III, Technical University of Denmark, 1978 (unpublished).
- 17) I. Goroff and L. Kleinman: Phys. Rev. 132 (1963) 2283.
- 18) M. Cardona in: "Atomic Structure and Properties of Solids", ed. by E. Burstein (Academic Press, N.Y. 1972) p. 514.
- 19) D. Olego, M. Cardona, and U. Rössler: Phys. Rev. in press.
- 20) M. Chandrasekhar, U. Rössler, and M. Cardona, Phys. Rev. in press.
- 21) F. Cerdeira, T.A. Fjeldly, and M. Cardona, Phys. Rev. B8, 4734 (1973).
- 22) H.R. Trebin, M. Cardona, R. Ranvaud, U. Rössler in: "Proceedings International Conference on Narrow Gap Semiconductors" (Polish Sci. Pub. 1978) p. 227.
- 23) K. Murase and S. Sugai: Solid State Commun. 32 (1979) 89.
- 24) N. Kristoffel and P. Konsin: Ferroelectrics 6 (1973) 3.
- 25) G. Abstreiter, A. Pinczuk, R. Trommer, and M. Cardona: Solid State Commun. 30 (1979) 703.
- 26) U. Novak, W. Richter, G. Sacks, and A. Stahl, to be published.
- 27) D. Olego and M. Cardona: Solid State Commun. 32 (1979) 375.
- 28) J.F. Scott: Solid State Commun. 9 (1971) 759.
- 29) P.A. Wolff: Phys. Rev. Letters 16 (1966) 225.
- 30) J.F. Scott: Advances in Physics, to be published.
- 31) A. Pinczuk, G. Abstreiter, R. Trommer, and M. Cardona: Solid State Commun. 30 (1979) 758.
- 32) V.A. Voitenko, I.P. Ipatova, and A.V. Subashiev in: "Light Scattering in Solids", ed. by Birman, Cummins, and Rebane (Plenum, N.Y. 1979) p. 83.
- 33) P.M. Platzman: Phys. Rev. 139A (1965) 379.
- 34) M. Chandrasekhar, M. Cardona, and E.O. Kane: Phys. Rev. 16 (1977) 3579.
- 35) M. Chandrasekhar, U. Rössler, and M. Cardona: Phys. Rev., in press.